

## VEHICLE DESIGN OF A SHARP CTV CONCEPT USING A VIRTUAL FLIGHT RAPID INTEGRATION TEST ENVIRONMENT

Fanny A. Zuniga<sup>\*</sup>, Susan E. Cliff<sup>\*</sup>, David J. Kinney<sup>\*</sup>, Stephen C. Smith<sup>†</sup>  
*NASA Ames Research Center, Moffett Field, CA 94035*

Veronica M. Hawke<sup>‡</sup> and Chun Y. Tang<sup>‡</sup>  
*ELORET Corp., Sunnyvale, CA 94087*

### Abstract

In an effort to improve the overall aerospace vehicle design process, a design environment that merges technologies from piloted simulations, computational fluid dynamics, wind-tunnel and flight test data is currently under development at NASA Ames Research Center. The specific objective of this project, entitled Virtual Flight Rapid Integration Test Environment, was to assess the role that piloted simulations can play in the conceptual design of advanced vehicles. As a result, a conceptual design study of a Crew Transfer Vehicle was undertaken to demonstrate this rapid turn-around process. This process included aerodynamic models generated from computational fluid dynamic methods, data validation from wind-tunnel testing, and a high fidelity pilot-in-the-loop motion-based flight simulation. These vehicles were designed using multi-point numerical optimization methods coupled with an Euler flow solver. A low-speed wind-tunnel test was conducted to validate the low-speed aerodynamics database. A piloted simulation experiment was conducted to evaluate the low-speed handling qualities of the various configurations in the approach and landing phase. Six astronaut pilots evaluated each of the configurations using Cooper-Harper ratings. The knowledge gained from the simulation data and pilot evaluations was quickly returned to the design team. From these findings, a new configuration was developed and cycled back through the simulation evaluation. This paper will summarize the design process of the Virtual Flight Rapid Integration Test Environment and discuss the results of the design study including the piloted simulation experiment.

### Introduction

The Virtual Flight Rapid Integration Test Environment (RITE) project was initiated to develop an

information technology process to rapidly and easily merge data from computational fluid dynamics (CFD), wind tunnel, and/or flight test into a real-time, piloted flight simulation. The process then cycles the knowledge gained from the simulation back into the design process. To accomplish this, a new engineering design environment was constructed that combined these various data generation methods and test environments within one infrastructure. The goal of this project was to develop such a design environment to improve current design methodologies and to reduce design cycle time. Current design environments do not allow data transfer and integration to take place easily between the different technologies during the preliminary design. By providing an infrastructure that brings together all these technologies, designers will be better equipped with higher-fidelity tools and methods, including simulation studies, which will lead to higher-fidelity preliminary designs.

The main advantage of conducting piloted simulation studies early is to identify problems and deficiencies in aerodynamic performance, vehicle stability and control, and guidance and navigation, which can be addressed in the preliminary design phase. Simulation studies also allow for the opportunity to develop preliminary control systems early in the developmental phase. Historically, the outer mold lines of a design are defined before simulation studies and control system development can begin which may lead to expensive and complex control systems and less than optimal vehicle performance. The Space Shuttle Orbiter<sup>1</sup>, which was designed in the 1970's, is an example of such developmental problems. More recent design studies have used simulation tools in the design phase but without an infrastructure and process in place to facilitate and expedite its use.<sup>2,3</sup>

Presently, the Virtual Flight RITE project has demonstrated the rapid and seamless integration of CFD, flight, and wind-tunnel data into a simulation database. During an early phase of the project, the Space Shuttle Orbiter was selected as the baseline configuration for this re-design demonstration. The radius and length of the nose of the Orbiter were altered as the design parameters. This phase of the project led

---

<sup>\*</sup> Aerospace Engineer, Senior Member

<sup>†</sup> Aerospace Engineer, Associate Fellow

<sup>‡</sup> Research Scientist

to a successful demonstration of integrating CFD, flight and wind-tunnel data into a simulation database for rapid preliminary design work. More recently, an integrated design process augmented by the RITE process was used to develop a viable conceptual design for a Crew Transfer Vehicle (CTV). The goal of this work was to develop an optimal design for a CTV while improving the tools and techniques of the RITE process.

CTV concepts are being studied as elements of various launch architectures under the 2<sup>nd</sup> Generation Reusable Launch Vehicle program. NASA Ames Research Center personnel developed conceptual designs for a candidate CTV which is presented here and in Reference 4. The primary mission objectives of the CTV included orbit-to-orbit transfer and rendezvous with the International Space Station (ISS). The Ames preliminary designs included the ultra-high temperature ceramic (UHTC) material<sup>5</sup>. This new UHTC material enabled the use of sharp leading edges and nose geometries during hypersonic flight. Historically, re-entry space vehicles have been designed using blunt-body concepts<sup>6</sup> to meet the temperature constraints of current thermal protection material. Because of unique structural, thermal and chemical properties, UHTC's are capable of nonabating operation approaching 5100 deg. F. Using this new material, designers were allowed to use sharp-bodied concepts in the conceptual designs. As has been reported<sup>4</sup>, sharp-bodied designs for reentry can greatly improve the crossrange, allowing significantly greater flexibility in selecting re-entry trajectories and landing sites. However, achieving good transonic and subsonic flight characteristics for this class of vehicle presented a challenge to the designers, which warranted the study of the approach and landing characteristics.

The RITE process was ideally suited for this design study because it provided the infrastructure needed for simulation studies to be integrated into this design process. For this reason, the CTV design was selected as the next case study under the RITE process. This paper will present the results of this study and process, which included vehicle design optimization, CFD, wind tunnel and a full-motion simulation experiment conducted in the NASA Ames Vertical Motion Simulator (VMS) facility. The objectives of this experiment were to evaluate the approach and landing flight characteristics of the CTV and to develop a control system optimization tool for use in the RITE process. Six astronaut pilots evaluated the handling qualities of the CTV configurations and for comparison purposes, also evaluated the handling qualities of the Space Shuttle Orbiter and NASA-Langley's HL-20<sup>7</sup> design. The details of this simulation experiment

and significant results will be summarized in this paper. This paper will also contain a detailed summary of the overall integrated design process including the RITE process used in developing a design for the CTV vehicle concept.

### Integrated Design Process

Various sharp-bodied design concepts for the CTV were developed for study using an integrated design framework developed under the High Performance Computing and Communication Program (HPCCP) and Information Technology (IT) Base Programs. This integrated design process was further augmented by the RITE process to evaluate concepts during approach and landing through piloted simulations. A summary of this integrated design process including the RITE process is outlined in Figure 1.

Initially, the configurations were designed using a Newtonian-based aerodynamic method in the hypersonic speed regime. Surface geometry was defined using the Rapid Aircraft Modeler (RAM)<sup>8</sup>, Pro-Engineer and Gridgen computer programs. Volume grids for the new geometry were generated using CART3D<sup>9</sup> for the unstructured, cartesian Euler solutions, MESH3D<sup>10</sup> for the unstructured tetrahedral Euler-flow solutions, and Gridgen for the structured Navier-Stokes flow solutions. Data generation methods included methods of various levels of fidelity including vortex lattice methods, Euler methods and

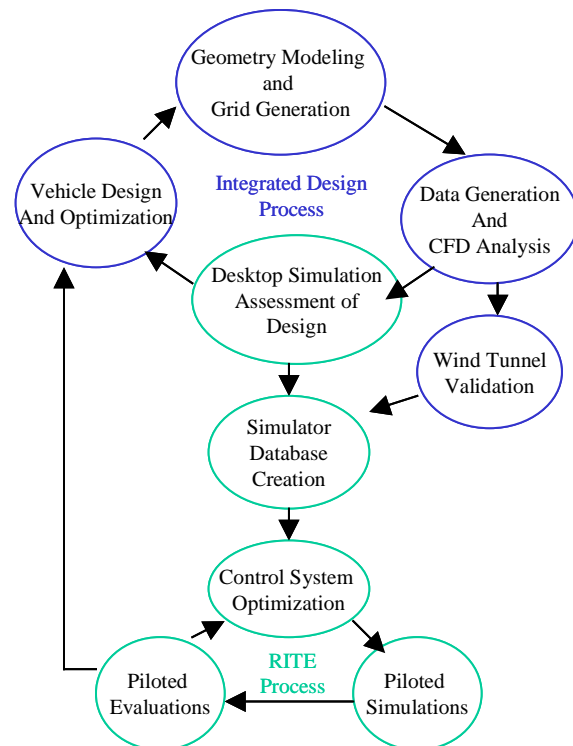


Figure 1. Flowchart of integrated design process

Navier-Stokes methods. The Euler solutions were computed using CART3D and AIRPLANE<sup>10-11</sup> while the viscous solutions were computed using Overflow-D<sup>12-13</sup>.

Stability and control dynamic derivatives were computed using VORVIEW<sup>14</sup>, a vortex lattice method. Wind-tunnel data were used for validating the low-speed CFD results.

Using these CFD data, a desktop simulation tool, using Matlab Simulink, was built and run to evaluate the trim and stability characteristics of the initial design configurations. In addition, a control system optimization tool, named CONDUIT<sup>15</sup>, was used to optimize the control system gains for each CTV configuration. From the results of these desktop simulation studies and CFD data analyses, a gradient-based design optimization method, QNMDIF<sup>16</sup>, coupled with AIRPLANE was used to improve the trim, stability and aerodynamic performance of the design in an iterative process.

From the results of these data generation methods, new math models for these configurations were developed and integrated for use in full-motion, 6-degree-of-freedom simulation studies in the NASA Ames VMS facility. Selection and integration of these different CFD datasets was initially done manually to determine all the steps involved in this process. These datasets contained different levels of fidelity, which warranted careful integration, and generation of the data. Information technologies were then applied to aid in the decision-making and automation of this data integration process.

Once the new math models were integrated into the VMS simulator's database, the handling qualities of each CTV configuration were evaluated using Cooper-Harper<sup>17</sup> ratings during the approach and landing phase. As shown in Figure 1, results from the handling qualities evaluations were fed back to the design team. Using this new information, a new vehicle configuration was developed and cycled back through the rapid re-design process. To demonstrate the speed of this process, a new configuration was developed after initial pilot evaluations and was completed within 4 weeks.

## Vehicle Design and Optimization

### Baseline Design

The baseline design for this conceptual study was based on a sharp-bodied vehicle design, designated CTV-v7. The conceptual design study of CTV-v7 and its earlier version named CTV-v5, are described in Reference 4. The tools used in developing these vehicles are also described in Reference 4. A hypersonic aerospace vehicle synthesis code (HAVOC)

was the main tool used in this design process. This tool used engineering analysis methods to compute vehicle performance and design characteristics, including aerodynamics and thermodynamics, propulsion, structures, trajectory and system cost. In the design process, the synthesis code converges the design to meet mission performance requirements.

The CTV-v5 and CTV-v7 adopted the same mission requirements as the NASA-Langley HL-20 design to allow a direct comparison between the blunt-bodied and sharp-bodied designs. While Reference 4 details these requirements, the major requirements are listed below:

1. Reusable
2. 8 passengers and crew
3. Launch on an expendable launch vehicle
4. Subsonic L/D greater than 4

The CTV-v7 design was further modified under this current study to improve its trim and stability characteristics. The CTV-v7 was renamed as Concept Vehicle 0 or CV0 to represent the baseline design for this current study. Future design configurations were deemed Concept Vehicles and increased in number sequentially. Figure 2 presents a 3-view and an isometric view of CV0.

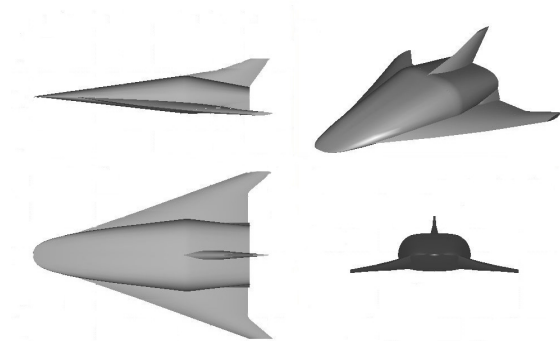


Figure 2. Baseline Vehicle Design, CTV-v7 (or CV0)

### Aerodynamic Shape Optimization

The Euler unstructured-tetrahedral-grid-based CFD code, AIRPLANE, was recently coupled to a gradient-based optimization algorithm, QNMDIF, to develop an aerodynamic shape optimization technique for the NASA Ames HPCCP. QNMDIF is an unconstrained quasi-Newton finite-difference optimization method. These codes were evaluated for the HPCCP program by applying the method to the current CTV conceptual design study. This method was used to optimize aerodynamic performance by varying selected geometry design variables for each Concept Vehicle design. In addition, manual design efforts were employed periodically for rapid exploration of

design variables and to limit the extent of shape changes made during optimization.

The resulting configurations (CV1 through CV5) from this optimization process were used for the approach and landing simulation database for the RITE project. The stability and control for this class of vehicle was particularly problematic since the vehicle needed to be trimmed from re-entry at hypersonic speeds to subsonic speeds for approach and landing. AIRPLANE was used for simultaneous optimization at Mach 6.0 (descent after re-entry) and Mach 0.3, (approach/landing speed). The design objective was to trim the vehicle at the two conditions simultaneously while achieving the best lift/drag (L/D) in the process.

#### CV1 Design

The design objective for CV1 was to modify the longitudinal stability so that the vehicle would be trimmed or nearly trimmed using ideal elevator deflections while simultaneously improving the performance of the vehicle at both design points. Wing twist, camber and elevator (inboard wing flap) deflection angle were the design variables. The wing flap angle was determined independently of the camber and twist design variables at the two Mach numbers, thus different geometries were analyzed at each design point during optimization. The two design points used for this optimization were 1) Mach 0.3 at angle of attack,  $\alpha = 9^\circ$ , and 2) Mach 6.0 at  $\alpha = 13^\circ$ .

The results showed substantial changes to the camber of the vehicle combined with  $-12.4^\circ$  of twist (wash out) to maximize the trimmed aerodynamic performance of the model. The optimized elevator deflection angles were;  $0.05^\circ$  (flap down) and  $5.2^\circ$  (flap up) for the Mach 0.3 and Mach 6.0 design points, respec-

tively. Figure 3 compares the twist about the trailing edge and airfoil modifications between CV0 and CV1. The AIRPLANE lift, drag and pitching moment coefficient ( $C_L$ ,  $C_D$  and  $C_m$ ) data for CTV configurations, CV0 through CV5, are shown in Figures 4 and 5 for Mach 0.3 and Mach 6.0, respectively. CV5 was designed during the VMS simulation experiment using simulation data and pilot feedback and is, therefore, described in a later section.

#### CV2 Design

One aspect of the CV1 design that was considered undesirable was an excessive amount of negative camber that leads to a concave upper surface. Therefore, the upper surface of the break section was modified manually to eliminate this concavity. As can be seen from Figures 4 and 5, the effect on the force and moment coefficients was minimal as expected. The moment coefficient was shifted slightly to the right (increased nose down moment) at Mach 0.3, and almost imperceptible at Mach 6.0 (Figures 4 and 5). At the hypersonic Mach numbers the pressures on the wing surfaces became nearly constant regardless of upper surface shape.

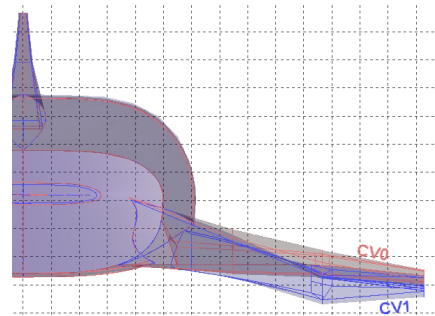


Figure 3. Comparison of CV0 and CV1

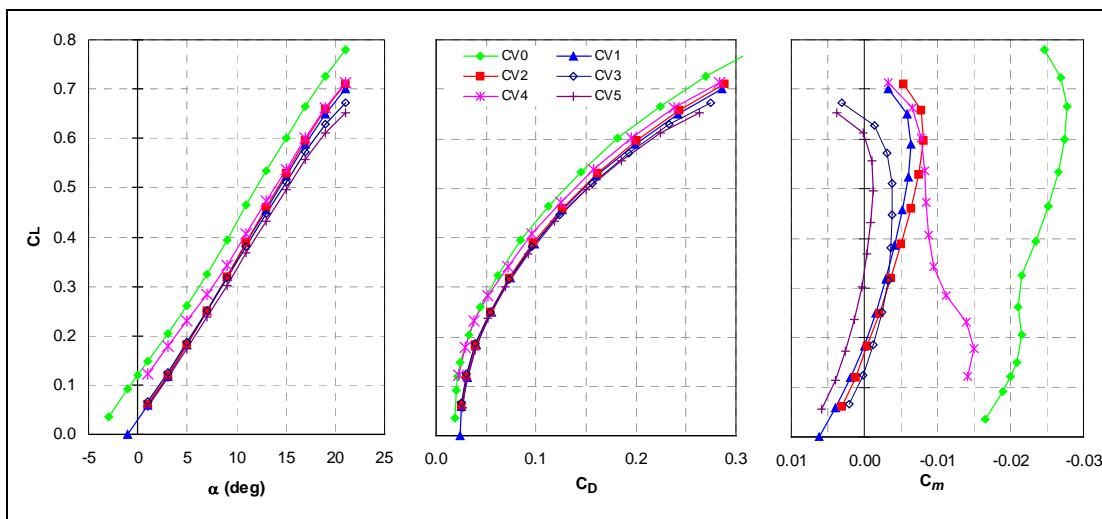


Figure 4. Mach 0.3 AIRPLANE Results

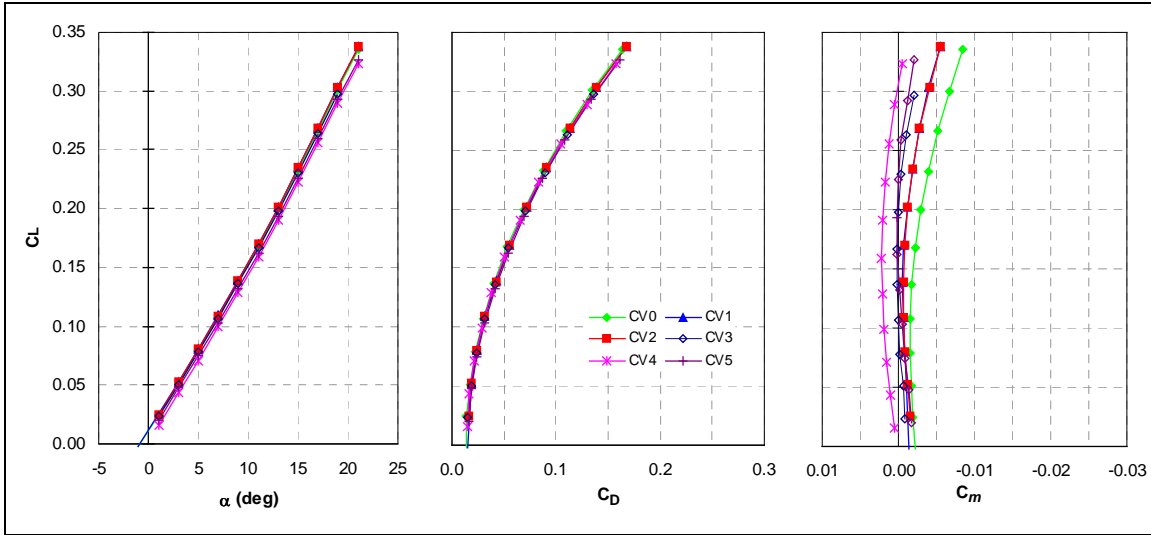


Figure 5. Mach 6.0 AIRPLANE Results

*CV3 Design*

The design of the CV3 configuration was done manually. The CV3 configuration consisted of the CV2 configuration with positive wing dihedral applied to the outer wing panel beyond the trailing edge break. The inclusion of wing dihedral was deemed necessary to stabilize the lateral-directional stability modes. A linear analysis was conducted on the preliminary aerodynamic data to determine the longitudinal and lateral-directional stability modes for all the CV configurations to date. The results of this analysis predicted dutch-roll mode instabilities for CV0, CV1 and CV2 for the open-loop dynamic system. Figure 6 shows the open-loop lateral-directional poles for CTV configurations CV0 through CV2 and CV3 with 30° and 45° dihedral.

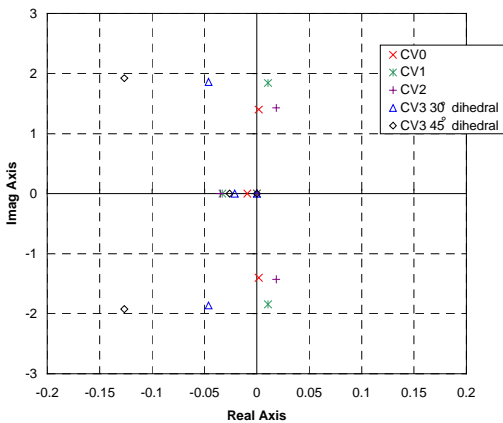


Figure 6. Lateral-directional poles for open-loop system for CV0 through CV3

This figure focuses in only on the poles near the imaginary axis where the problem occurred and does not show the poles to the far left. As can be seen

from the figure, the open-loop poles of CV0 through CV2 are on the right-hand side of the real axis and, hence, are unstable. This instability increased from CV0 to CV2. With the addition of dihedral, the open-loop poles moved to the left or stable side of the real axis as shown in the figure. The 45° dihedral case resulted in complex poles more stable than the 30° dihedral case; however, its poles on the real axis were seen to be less stable than the 30° dihedral case.

Figure 7 compares the untrimmed pitching moment characteristics at Mach 0.3 between the CV3 dihedral cases and CV0 through CV2. As can be seen from this figure, the effect of the 30° dihedral case caused the pitching moment curve to become less stable above a  $C_L$  of 0.3 to a  $C_L$  of 0.6. This effect was even more dramatic for the 45° dihedral case. Based on these two figures, it was decided that the 30° dihedral

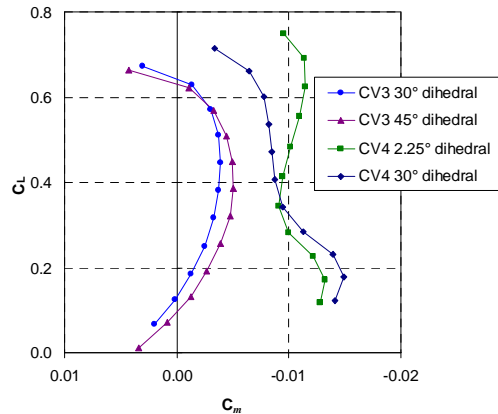


Figure 7. Untrimmed pitching moment characteristics at Mach 0.3 for 30° and 45° dihedral

case would yield better results and, therefore, the CV3 configuration was defined to be CV2 with 30° dihedral.

Figure 8 compares the outboard dihedral change between CV2 and CV3. The force and moment coefficients are compared in Figures 4 and 5. A positive aspect to the addition of the wing dihedral is that the vehicle can easily be trimmed for a wider range of lift coefficients. The effect of the wing dihedral at Mach 6.0 shows a similar rotation of the moment curves. Neutral stability is also seen for fairly wide range of lift coefficients (0.075 to 0.225).

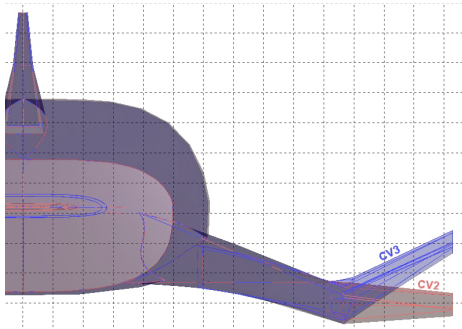


Figure 8. Wing dihedral change between CV2 and CV3

#### CV4 Design

The design of the CV4 configuration was performed using AIRPLANE optimization of the CV0 configuration. This design permitted small changes in the planform of the vehicle, whereas all previous designs did not. The design variables included wing twist about the leading edge rather than the trailing edge since the previous CV1 design developed substantial outboard leading edge droop from trailing edge twist, twisting about the leading edge would likely raise the trailing edge up. Other design variables included wing sweep and wing dihedral. The sweep was limited to  $\pm 2$  inches while the dihedral was limited to  $\pm 2.2$  in. of vertical movement during optimization.

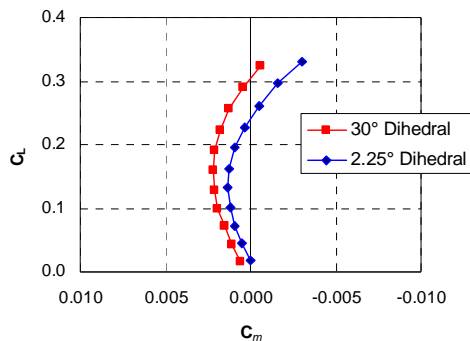


Figure 9. Untrimmed pitching moment characteristics for CV4 at Mach 6.0 at 30° and 45° dihedral

The pitching moment coefficient results of optimization with the objective function for the two design points at Mach 0.3 and Mach 6.0 are shown in Figures 7 and 9, respectively. The dihedral angle obtained from optimization was only 2.25°. These results showed the vehicle trimmed at Mach 6.0, but not trimmed at Mach 0.3 for this dihedral angle.

The rolling ( $C_l$ ) and yawing ( $C_n$ ) moment coefficients were assessed for this vehicle at Mach 0.3 and are presented in Figure 10. The magnitude of the rolling moment was determined to be too small for the optimized dihedral angle of 2.25°. Thus, to increase the magnitude of the rolling moment coefficient, the wing dihedral was increased to 30° to match that of the CV3. This increase in dihedral made the rolling and yawing moments equal and opposite which was desirable. However, the increase in dihedral had a negative effect on the pitching moment curves. As can be seen in Figures 7 and 9, the Mach 0.3 moment curve was rotated so that the vehicle was no longer statically stable and the trimmed Mach 6.0 vehicle now had a positive, nose-up pitching moment, respectively.

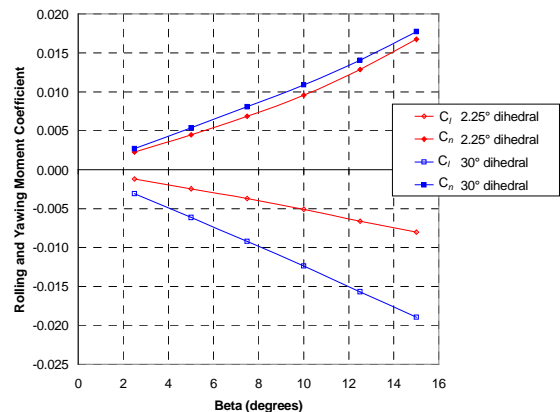


Figure 10. CV4 rolling and yawing moment coefficients at Mach 0.3 for angle of attack of 10°

The design team decided that the rolling and yawing moments being equal and opposite with the 30° of dihedral outweighed the adverse affects on the trim and stability at both Mach numbers. In addition, the team was interested in the challenge of achieving a vehicle with good handling qualities via the control system optimization process for this design. Thus, the CV4 configuration included the 30° dihedral.

The resulting changes to the planform as compared to the CV3 configuration are shown in Figure 11. Figure 12 shows the resulting changes to the wing design also compared to the CV3 wing design. Finally, comparison of the CV4 force and moment coefficients

ients to the other CV configurations is shown in Figures 4 and 5.

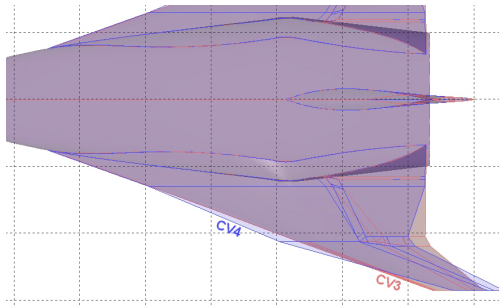


Figure 11. Wing planform changes to CV4

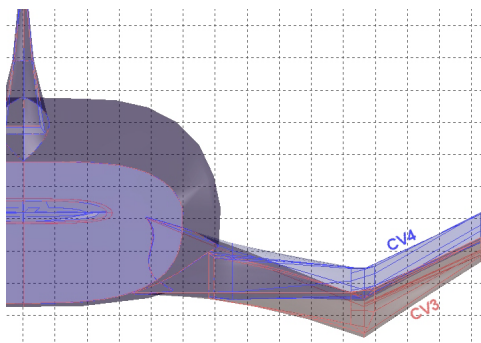


Figure 12. Wing modifications to CV4

#### HL-20 Vehicle

In addition, the HL-20 geometry configuration was used as a blunt-body comparison to the sharp-body vehicle designs. The HL-20 was developed at NASA-Langley as previously mentioned and designed to meet the same mission requirements as the sharp-bodied CTV designs. Figure 13 below pictures the geometry of the HL-20. Figure 14 compares the untrimmed aerodynamic data of the HL-20 with that of the Space Shuttle Orbiter and CTV configurations (CV0 through CV3) at Mach 0.3.

HL20 model

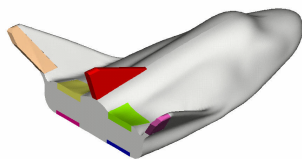


Figure 13. NASA Langley's HL20 vehicle

#### Wind-Tunnel Test

As part of the design process, low-speed wind tunnel tests of the CV0 and CV2 configurations were performed in the NASA Ames Fluid Mechanics Lab 3-foot by 4-foot indraft wind tunnel. A detailed de-

scription of the wind tunnel geometry and performance is provided in Reference 18.

The wind-tunnel model was fabricated from a polyester resin using a stereo lithography technique. The

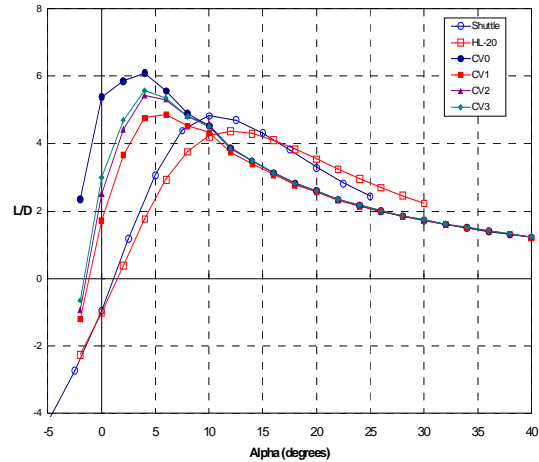


Figure 14. Comparison of untrimmed aerodynamic data at Mach 0.3 for Space Shuttle Orbiter, HL-20 and CTV configurations

wings of the CV0 and CV2 were attached to a common fuselage. Inboard and outboard elevons and rudder control surfaces were modeled as separate, removable components to represent various control surface deflections. Figure 15 below illustrates the wind-tunnel model of CV0.

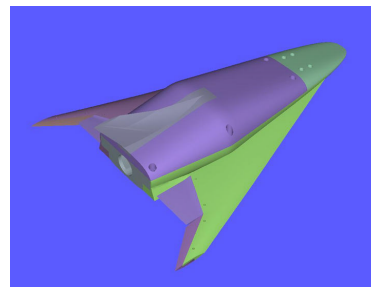


Figure 15. Wind-tunnel model of CV0

The model was mounted on a sting-type support through the flat base of the model. A six-component force balance and 3-axis accelerometer was mounted inside the model for force and moment and angle-of-attack measurements, respectively. For these tests, the wind tunnel was operated at a dynamic pressure of 20 psf, which resulted in a Mach number of 0.11 and Reynolds number of 1.1 million based on a body length of 22 inches. Data were taken over a range of angle of attack from  $-3^\circ$  to  $22^\circ$ , and a range of side-slip angles from  $0^\circ$  to  $5^\circ$  at  $0^\circ$  angle of attack. During the testing, each configuration was tested inverted as well as upright to determine wind tunnel stream angle correction. No blockage or wall-effects correc-

tions were made to the data. A representative sample of the wind-tunnel data for the CV0 configuration is shown in Figure 19. Comparisons to the CFD results are also shown in this figure and discussed in the following section.

#### Data Generation and Integration

Once the CTV geometries (CV1 through CV4) were defined using the aerodynamic shape optimization technique described previously, various data generation methods were employed to develop an aerodynamic database for each CTV configuration. These databases were developed for integration into the full-motion, 6-degree-of-freedom simulation in the VMS for approach and landing studies. The data generation methods consisted of Euler solvers (AIRPLANE and FlowCart), a Navier-Stokes solver (Overflow-D) and a vortex lattice method (VORVIEW).

#### Geometry Modeling and Grid Generation

Each CTV geometry was transferred to the RAM program at the end of the aerodynamic shape optimization process. The RAM program is a tool for quickly defining geometry for aerospace vehicles and exporting data for use in grid generation. At the end of the aerodynamic shape optimization process, the changed geometry sections were entered manually into the RAM program. RAM then re-lofted the wing with the new sections. Once in the RAM program, the geometry file was automatically transferred into a grid generation package. By the end of CV4, an automated process was developed to directly transfer the geometry files from AIRPLANE to the CAD packages.

All CTV CAD databases were generated in Pro/Engineer (ProE) 2000i. ProE was the CAD system of choice because of its parametric design capability. After the geometry from RAM was imported into ProE, the gridding software, Gridgen was used to generate the surface grids. Gridgen read the CAD database in IGES format, which ProE converted to its own file format. Beginning with the baseline, CV0 model, a basic grid topology for Overflow-D was developed to simplify and expedite future geometry changes to the models.

Figure 16 shows the symmetry plane of a typical unstructured Cartesian grid used in the Euler (FlowCart) calculations. Similarly, the symmetry plane and surface overset structured grids created for the Navier-Stokes solver are illustrated in Figure 17. Finally, the symmetry plane of the AIRPLANE tetrahedral grids is illustrated in Figure 18. In comparison to Figures 16 and 17, the AIRPLANE grid showed a smooth gradation from the surface to the farfield boundary.

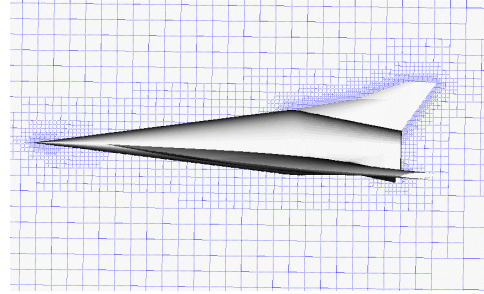


Figure 16. Unstructured Cartesian Grid

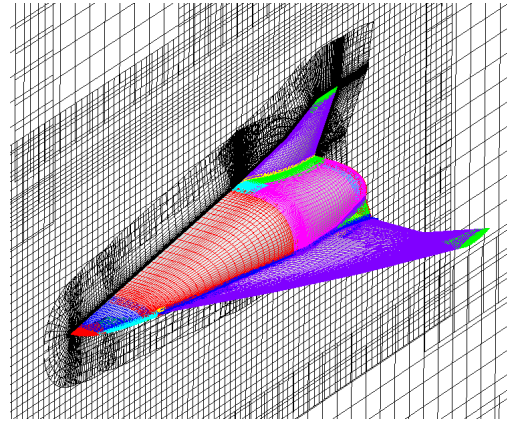


Figure 17. Overset Structured Grid

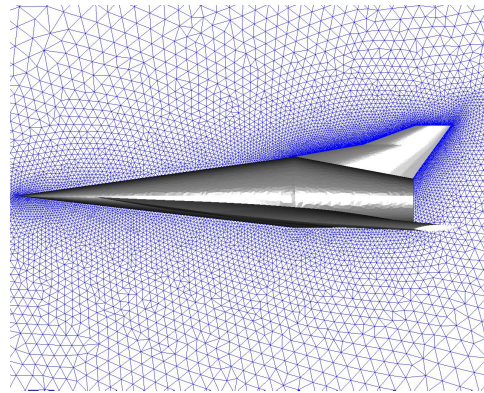


Figure 18. AIRPLANE Tetrahedral Grid

#### Data Generation using CFD codes

The first step in the data generation process was the selection of appropriate CFD codes. Ideally, all data generated would use the highest fidelity code available which implies that only Navier-Stokes (N-S) simulations would be computed. However, this is not feasible because these calculations are very time consuming. Hence, the choice of a particular solver is usually a tradeoff between accuracy and turnaround time. Under the RITE process, a combination of N-S and Euler simulations were used for the creation of the simulator aerodynamic database. The N-S solver

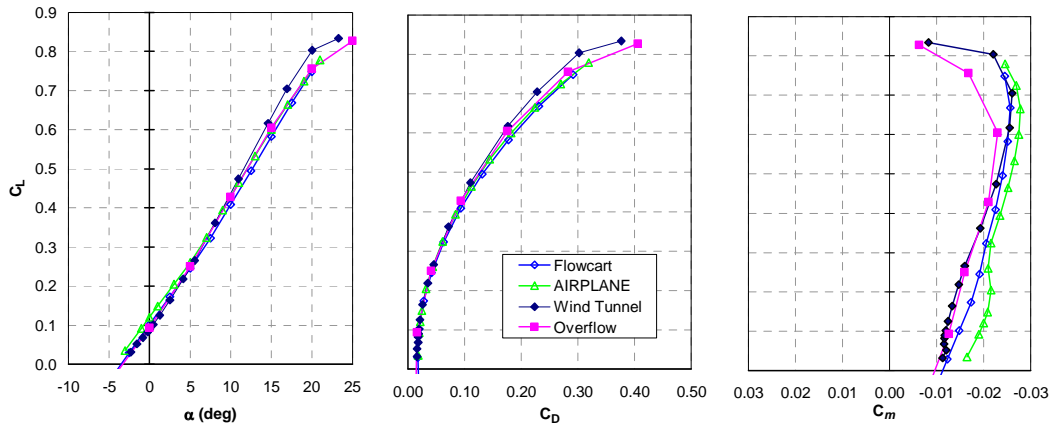


Figure 19. Baseline CTV (CV0) configuration, Mach $\leq$ 0.3

used for these computations was Overflow-D and the Euler solvers used were FlowCart and AIRPLANE.

Figure 19 compares the differences in the force and moment coefficients computed for the various CFD codes used. As mentioned previously, the Euler solver, AIRPLANE, was coupled with an optimizer to maximize the performance characteristics of the configurations. Once the configurations were optimized, the Euler solver, FlowCart, was used to expedite the data generation process. The figure shows good agreement between these two Euler solvers. Figure 19 also shows good agreement between the N-S, the Euler solvers and the wind-tunnel data for  $\alpha \leq 10^\circ$ , except for the pitching moment coefficients.

At higher  $\alpha$ , the differences between the N-S and wind-tunnel data can be attributed to several factors including differences in Reynolds number, turbulence modeling, model sting correction and small-scale effects. The N-S solver was run using a Reynolds number of 0.5 million/ft. and the wind tunnel was run at a Reynolds number of 0.6 million/ft using a 5%-scale model. These findings indicated that further study was needed to resolve the differences in the data. However, the wind-tunnel test was run very late in this integrated design process and no further studies could be undertaken prior to the simulation experiment. Therefore, the N-S data was used for most of the data integration process.

In addition to static forces and moments, the motion simulator also needed dynamic coefficients to model the vehicle. VORVIEW was selected for this task because it was the only tool capable of computing these quantities in a reasonable amount of time. It is unknown how well VORVIEW predicted these coefficients since no wind tunnel data or other CFD results were available for a comparison. A check of the dynamic coefficients estimated using VORVIEW on

the HL-20 with data from NASA Langley showed some differences in some of the quantities. Clearly, a study to assess the accuracy of VORVIEW and the accuracy required for the simulator is warranted. Alternative methods of computing dynamic derivatives (such as modifying FlowCart or running unsteady simulations using Overflow-D) are currently being evaluated in the next phase of the project.

#### Data Integration

The integration of data was very straightforward. Although many sources of data were available, the aerodynamic database was constructed mainly from the N-S results. No attempts were made to merge the wind tunnel data with CFD solutions. As discussed previously, there was insufficient time for careful study of these results to integrate into the database.

The CTV configurations (CV0-CV4) without deflected control surfaces were modeled using Overflow-D. The N-S simulations of deflected control surfaces were computed only on the baseline vehicle (CV0). These results were then extrapolated to the other CTV configurations when constructing the aerodynamic database. The Euler results consisted of the deflected speedbrake (split rudder) and ground effect cases. Finally, the VORVIEW results were integrated into the database which consisted of the dynamic derivatives. Table 1 lists the range of flow conditions and control surface deflections computed for this database.

Table 1. Range of conditions for computational data

Mach number	0.3 to 0.9
Angle of attack	$-10^\circ$ to $50^\circ$
Sideslip angle	$0$ to $20^\circ$
Inboard flaps	$-20^\circ$ to $20^\circ$
Outboard flaps	$-20^\circ$ to $20^\circ$
Rudder	$0$ to $20^\circ$
Speedbrake	$0$ to $30^\circ$

Initially, the ground effects model from the HL-20 model was extracted and integrated into the CTV aerodynamic databases. Results from the simulation experiment indicated that this model was not adequate. Feedback from the pilots indicated that these effects were not realistic enough for handling qualities evaluations. Consequently, Euler calculations using FlowCart were computed to develop a new ground effects model and compared with AIR-PLANE computations with good agreement.

### Control System Design and Optimization

A preliminary control system and linear aerodynamics model were initially developed and evaluated using desktop simulation tools (Matlab and Simulink). The HL-20 control system was used as a starting point for the CTV control system. This control system was modified to account for the control surfaces used on the CTV configurations. Figures 13 and 20 illustrate the HL-20 and CV1 configurations, respectively, with the control surfaces accentuated in color. As can be seen from the figures, there were major differences between the HL-20 and CTV control surfaces.

For the CTV configuration (Figure 20), the two inboard flap surfaces were designed for pitch control and trim. The size of these flap surfaces and alternate control surfaces were explored for best trim performance. The baseline vehicle, CV0, was originally designed with 20% chord flaps. In addition to increasing the size of this control surface, body flaps, leading edge slats and flaperons were all evaluated as

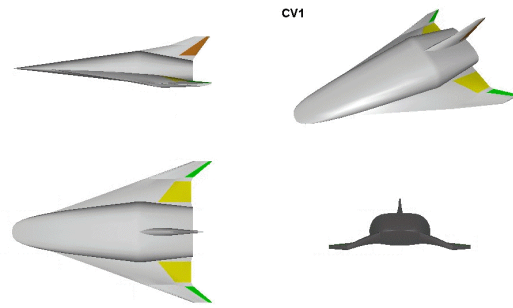


Figure 20. Control surfaces of CV1 configuration

trimming devices. As a result, the 30% chord inboard flaps were determined to give the best trim performance. These 30% flaps were used on CV1 as shown in Figure 20 and all subsequent Concept Vehicles.

Referring to Figure 20, the two outboard surfaces were used as ailerons for roll control and the rudder surface was used for directional control. A split rudder surface was used as a speedbrake for speed control on approach and landing. These control surfaces were used for all the CTV configurations.

The CTV preliminary control system was implemented into a full-motion 6-degree-of-freedom simulation in the NASA Ames VMS facility. The control system, aerodynamics and trajectory performances were initially evaluated during the build-up period in fixed-base operation. The initial simulation studies, conducted on CV0, revealed the following deficiencies: inadequate trimming capability, insufficient longitudinal control power and lateral-directional

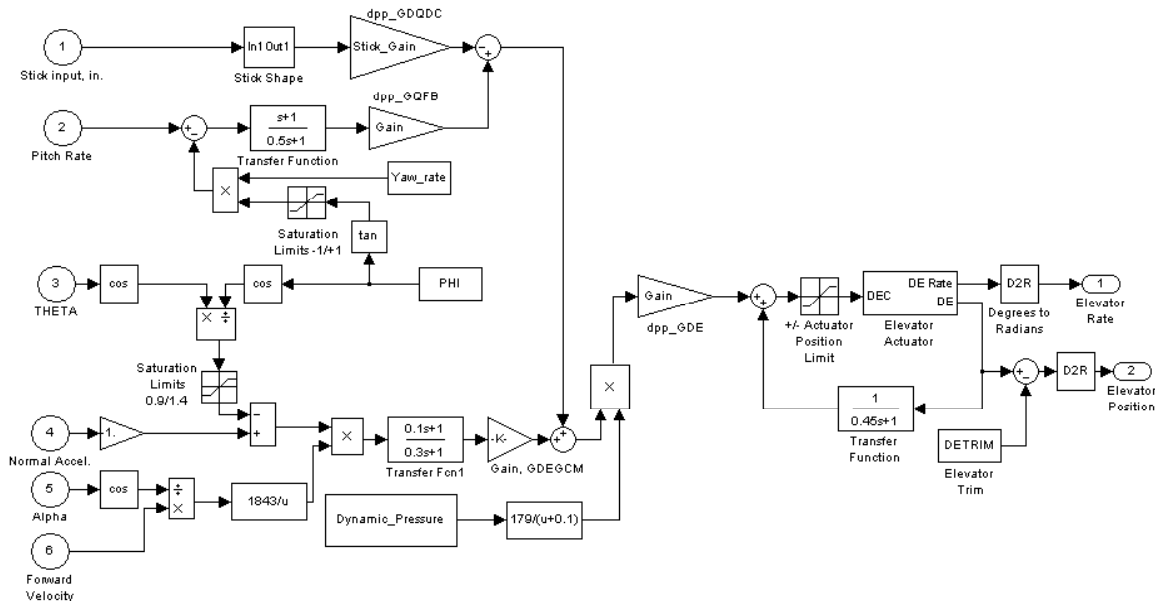


Figure 21. CTV Longitudinal Pitch Control Laws

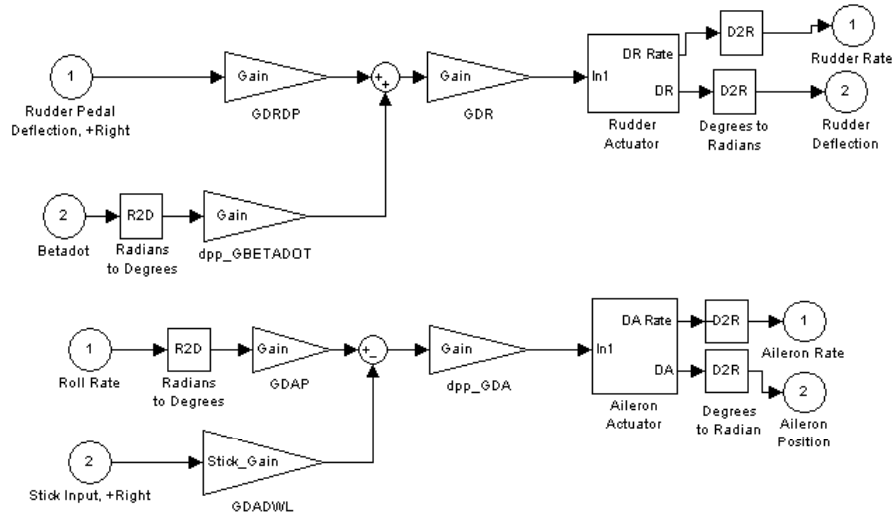


Figure 22. CTV Lateral-Directional Control Laws

instability. As a result of these initial studies, new Concept Vehicle configurations were developed to address these deficiencies. As described previously, flap size was increased to the design of CV1 for better trim performance and wing dihedral was added to CV3 for better lateral-directional stability.

Figures 21 and 22 present the longitudinal and lateral-directional control system architectures used for all the CTV configurations. Initially, the directional control law consisted of a yaw-rate damper in the feedback loop of the yaw channel. From initial pilot evaluations, this control law was found to be inadequate and at times unstable for the approach and landing tasks.

Alternate feedback control schemes were explored to improve the directional control. As a result, beta-dot feedback was determined to yield improved handling qualities for directional control. This feedback system is shown in Figure 22 and was used for all the CTV configurations.

For each of the Concept Vehicles, new aerodynamics models were generated and implemented into the simulation. New control system gains were optimized for each new aerodynamics model, corresponding to CV0 through CV4, using CONDUIT. A linear model of the vehicle dynamics was developed and implemented for use with CONDUIT. The model was verified against the 6-degree-of-freedom simulation using dynamic checks. In addition to optimizing control system gains, the optimization tool also predicted handling qualities levels from user-defined handling qualities and flight control system specifications. These specifications can be defined by the user or selected from CONDUIT's libraries of standard fixed- and rotary-wing specifications. When

optimizing in CONDUIT, the program tries to achieve the best or Level 1 handling qualities for the selected specifications by varying the user-defined design parameters. Since this was the first time using CONDUIT for this particular application, a major goal of the optimization process was to determine the best combination of handling qualities specifications and design parameters to be used consistently for all the CTV configurations.

Figures 23 and 24 show the longitudinal and lateral-directional handling qualities specifications used in the final evaluation of each CTV configuration. Each specification or block has 3 levels of compliance, as shown. The blue region defines the Level 1 handling qualities. The magenta region defines the Level 2 and the red region defines the Level 3 handling qualities. The different symbols in Figure 23 represent the different size input steps used for the pitch loop. The arrows in figures indicate the values are beyond the scale of the figure.

Initially, longitudinal and lateral-directional specifications for a fixed-wing vehicle of similar class and mission to the CTV were selected from the military specifications library included in the CONDUIT software. Although the results from CONDUIT showed Level 1 handling qualities for all the selected specifications, pilot evaluations from the full-motion simulation resulted in Level 2 and 3 handling qualities for all the CTV configurations. Much work was done during the VMS simulation to re-define the specifications used in the CONDUIT optimization process. These military specifications<sup>19</sup> were defined for large, heavy class vehicles similar in size to the CTV but for higher L/D performance than the CTV. Therefore, new specifications were needed for a re-entry space vehicle like the CTV.

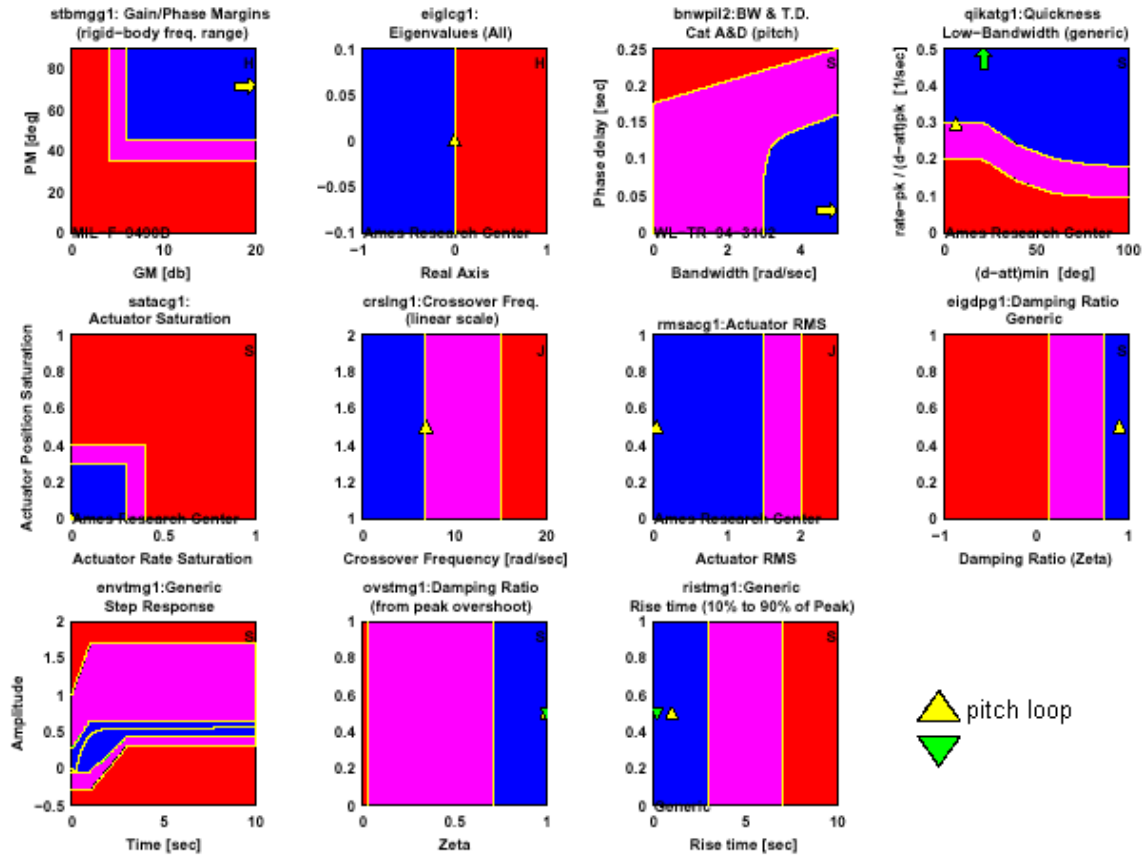


Figure 23. Longitudinal Handling Qualities Specifications from CONDUIT

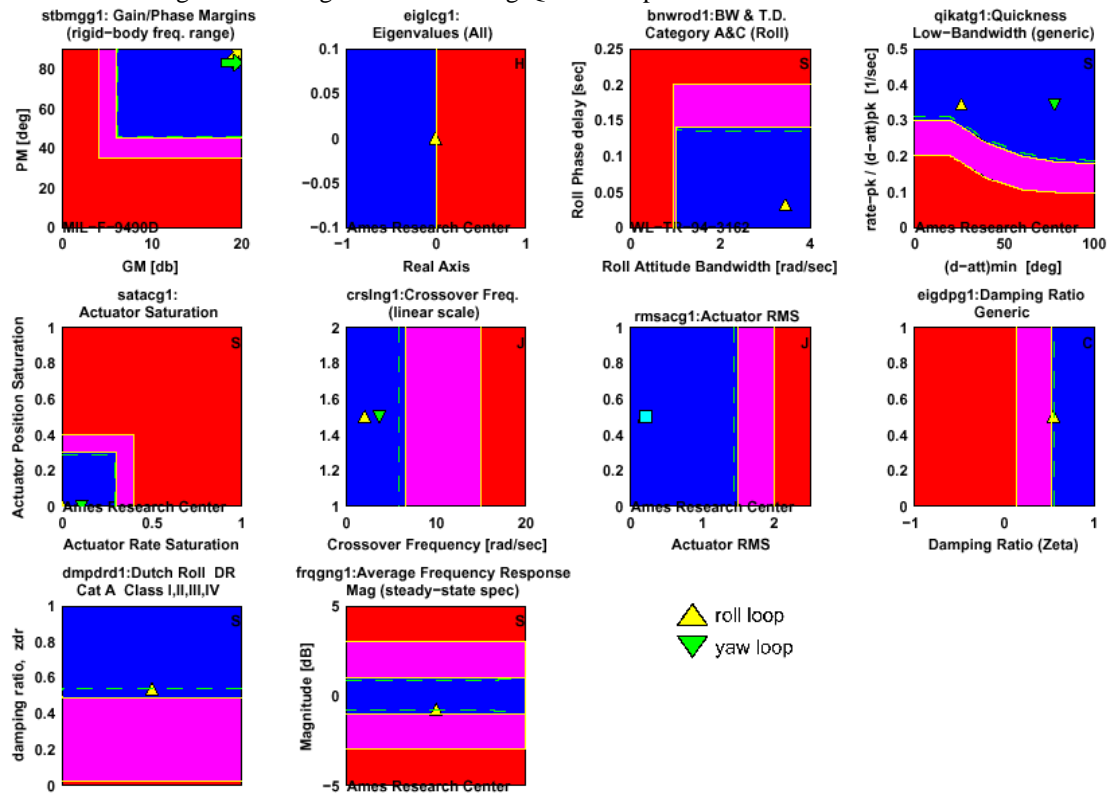


Figure 24. Lateral-Directional Handling Qualities Specifications from CONDUIT

After several iterations of obtaining pilot evaluations and re-defining the specifications, a good set of handling qualities and flight control system specifications were achieved. In order to obtain good results, the boundaries between the Level 1 and 2 regions for the longitudinal crossover frequency and damping ratio specifications were altered. As a result, much higher damping specifications and crossover frequencies than the military specifications were achieved as shown in Figures 23 and 24.

In addition, a good set of design parameters were also achieved. These design parameters, or in this case the control system gains are shown with prefixes *dpp\_* in Figures 21 and 22 for the longitudinal and lateral-directional control systems. This final combination of specifications and design parameters were used for all the CTV configurations. In this way, each new CTV configuration was quickly evaluated during the full-motion simulation without laboriously fine-tuning each control system gain and conducting a time- and frequency-domain dynamic analysis. The results of the handling qualities evaluations are discussed in the next section.

### **VMS Simulation Experiment**

A piloted simulation experiment of each of the CTV configurations in the approach and landing phase took place during a 4-week window in the NASA Ames VMS facility.

#### *Experiment Setup*

Full 6-degree-of-freedom simulations for each of the 6 CTV configurations (CV0 through CV5) were built and validated for this experiment. The CV5 configuration was designed, integrated and flown during the simulation experiment. The rapid re-design process of the CV5 configuration is described in a later section.

The HL-20 simulation originated from NASA-Langley and was transferred and integrated into the VMS simulation. The Langley simulation was also a 6-degree-of-freedom, full-motion simulation. In addition to dynamic check comparisons made between the HL-20 simulations, the simulation in the VMS was checked out and verified by NASA-Langley HL-20 pilot, Robert Rivers<sup>3</sup>. With the help of Rivers, the VMS HL-20 simulation was tuned and adjusted to match the Langley HL-20 simulation.

The Space Shuttle Orbiter simulation was taken from the existing VMS simulation of the Orbiter and was used without modification. This VMS simulation of the Orbiter is considered a high-fidelity simulation and is currently used for astronaut training and space shuttle engineering studies. In addition, the same cab

and hardware from the Orbiter simulation was used for the HL-20 and CTV simulations. Only the software was changed between each simulation. It took approximately 5 to 10 minutes to make the changes between simulations.

Each simulation consisted of an aerodynamic model, trajectory and guidance algorithms, control system architectures, HUD and graphics displays. For each CTV configuration, a function table was generated consisting of the aerodynamics data.

The experiment also took advantage of the virtual laboratory (VLAB) capability available in the VMS facility. This VLAB was developed to provide real-time transmittal of data, voice and graphics displays throughout the simulation to researchers off-site. The VLAB was used throughout the simulation to facilitate the exchange of information and data between the various technology groups at different sites at NASA-Ames and for demonstration purposes at NASA-Johnson and Marshall Space Flight Centers.

#### *Piloted Tasks*

The main task during the simulation was to approach and land from the Heading Alignment Cone (HAC) and 10K ft. initial conditions on to Kennedy Space Center (KSC) runways in wind and turbulent weather conditions. Other tasks included pitch, roll and rudder maneuvering tasks in air and during rollout. Three-axis doublets were also performed to evaluate the open-loop and closed-loop dynamic response of the vehicle.

For the handling qualities evaluations, the test matrix was narrowed down to three piloted tasks. These tasks included: 1) a nominal landing, 2) a lateral offset landing, and 3) a crosswind landing. All tasks were initiated at 10K ft. After the first landing, the pilot had the option to request a 5K ft. initial condition. For the nominal landings, the pilot was instructed to follow the guidance marker all the way down to touchdown. The guidance marker followed a 17° glideslope or 300 knots approach speed for the Orbiter and HL-20. The target touchdown speeds for the Orbiter and HL-20 landings were 195 kts. and 200 kts. respectively. The approach and target touchdown speeds for the CTV configurations were 200 kts. and 160 kts. respectively. This resulted in a 12° glideslope angle on final. Because of the higher L/D of the CTV as shown in figure 14, the pilot was capable of approaching and touching down at desirable slower speeds. Several other touchdown speeds were evaluated for the CTV configurations. It was determined that 160 kts. was the slowest speed that could be achieved without affecting the handling qualities ratings.

During the lateral offset tasks, the pilot was instructed to follow the guidance marker all the way down to 3000 ft. altitude. At this point, the pilot was instructed to make a sharp, abrupt right turn to a landmark approximately 400 ft. away from the centerline and follow this new alignment down to 300 ft. altitude. Then the pilot turned back towards the runway and proceeded to land on the centerline. This task was designed to be an aggressive maneuver to excite the lateral-directional modes to uncover any deficiencies in the control and dynamic systems.

The crosswind landings were evaluated in 20 kt. crosswinds. These were realistic winds taken from the Orbiter's simulation database of wind profiles measured at KSC and Edwards Air Force Base landing sites. These winds were then extrapolated to give 20 kts. of crosswind. The components of the winds used for the crosswind landing evaluations were 15 kts. tailwind and 20 kts. left crosswind.

#### *Piloted Evaluations*

Six astronaut pilots, including three flight-experienced Shuttle commanders, and one NASA-Langley HL-20 pilot participated in the experiment and handling qualities evaluations. The pilots provided valuable information and insight to the development of the simulation and design modifications to the CTV.

In addition to the piloted tasks described previously, the pilots were instructed to land within desired criteria when assigning Cooper-Harper ratings. The landing criteria are outlined in Table 2 below.

Table 2. Landing criteria for Cooper-Harper Ratings

<u>Parameter</u>	<u>Desired</u>	<u>Adequate</u>
Y touchdown	+/- 10 ft.	+/- 20 ft.
Touchdown speed	+/- 7 kts.	+/- 12 kts.
Altitude rate	<3.5 ft/sec	<5.0 ft/sec

Based on these criteria and the Cooper-Harper scale, the pilots were instructed to rate the handling qualities of each vehicle. In addition, the pilots were instructed to perform at least 2 repeat runs before assigning their ratings. These guidelines were followed by all the pilots for all the simulation evaluations.

Figure 25 presents the final Cooper-Harper ratings (CHR) for the Orbiter, HL-20 and the CTV Concept Vehicle configurations (CV0 through CV5). This figure shows averaged piloted ratings for each of the 3-piloted tasks described previously in the last sub-

section. The ratings were averaged over all the pilot ratings for the specified piloted task and vehicle configuration. Using the CHR scale, ratings 1 through 3 (with CHR of 1 being the best rating) are defined as Level 1 handling qualities. Ratings 4 through 6 are defined as Level 2 handling qualities while ratings 7 through 9 are defined as Level 3 handling qualities.

The handling qualities ratings for the CTV configurations in Figure 25 were taken using the final set of control system gains obtained with CONDUIT. As described in an earlier section, a good combination control system and handling qualities specifications along with selected design parameters were required for CONDUIT to achieve optimal control system gains and Level 1 handling qualities. Throughout the simulation, the pilot handling qualities were compared to the predicted handling qualities of CONDUIT. Initial comparisons resulted in poor correlations between the pilot ratings and CONDUIT. Although the CONDUIT program predicted Level 1 handling qualities, the pilot handling qualities for the CTV configurations ranged from Level 2 to Level 3 handling qualities.

Throughout the simulation experiment, pilot feedback was used to make changes in the control system architecture, trajectory and guidance algorithms, HUD displays and control system optimization specifications for improved performance in handling qualities ratings. As a result, good correlations were finally obtained between pilot ratings and CONDUIT for the CTV configurations. These pilot ratings improved from Level 3 to Level 1 ratings for 5 of the 6 CTV configurations (CV0 through CV3 and CV5) as shown in Figure 25. The handling qualities for CV4 as shown in the figure did not use this final combination of specifications in CONDUIT. Due to the time constraints of the pilots' schedules, the simulation experiment ended before this final evaluation could be made.

The CTV pilot ratings of Figure 25 were much lower than the pilot ratings of the Orbiter and HL-20 for similar tasks except for CV4. The pilots' comments also reflected and confirmed these good ratings. From a comparison of the CTV ratings, CV3 is shown to have the best overall ratings. However, one cannot immediately conclude that the CV3 configuration was the best overall configuration. More analysis is required to determine the control power used in achieving each task.

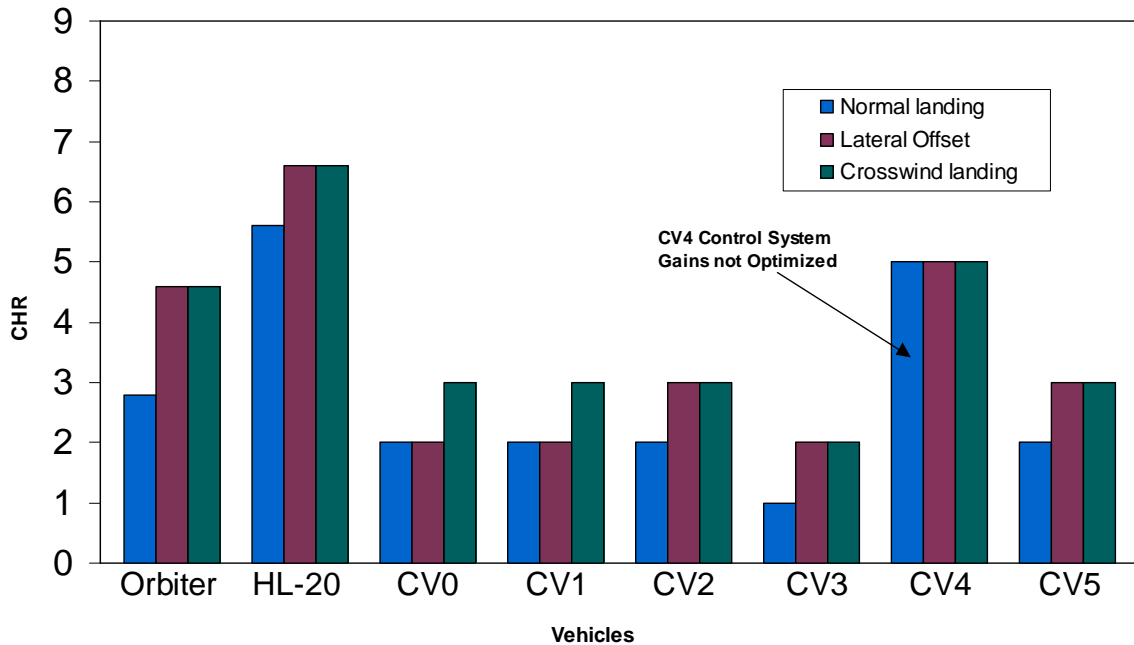


Figure 25. Summary of Cooper-Harper Ratings for all Vehicles

#### Rapid Redesign of CV5

The simulation experiment was also successful in demonstrating the capability to rapidly re-design a configuration using pilot feedback. During this rapid redesign process, a new aerodynamics model was generated and implemented into the full-motion simulation, control system gains were re-optimized and new pilot evaluations were obtained on the new design. A sixth configuration (CV5) was generated and evaluated using this rapid process during the simulation experiment.

From pilot feedback and recommendations, fuselage geometry variables were optimized to increase fuselage width and nose droop. Increasing these variables would improve the design by increasing fuselage volume and improving pilot visibility. Poor pilot visibility on this vehicle was a limiting factor in selecting a touchdown speed and contributed to the handling qualities ratings on landing. As mentioned previously, the touchdown speed for the CTV configurations was 160 kts. which required an angle-of-attack of approximately  $12^\circ$ .

Preliminary evaluations of CV0 through CV3 led the pilots to choose CV3 as the one with the best handling qualities of the 4 designs. Thus, CV3 was used as the baseline configuration for the rapid redesign case. The goal was to further improve the performance and handling characteristics of the CV3 configuration by applying small shape changes to the body, and allowing the wing to be re-twisted.

Seven design variables were used. These included wing twist about the leading edge applied at the tip and lofted to the side of body. The remaining 6 design variables were applied to the fuselage. These variables were body leading and trailing droop, forebody camber, and forebody upper surface thickness.

The resulting fuselage change to CV5 is shown in Figure 26. The difference in the fuselage can be easily seen by this side view. The nose was moved up 1.2 percent, and the aft body was drooped 3.2 percent. The wing twist about the leading edge was  $-2.293$  degrees (further washout). The forebody thickness was increased at 25% and reduced at 60% of the forebody. These forebody thickness changes were the most pronounced changes seen in the model.

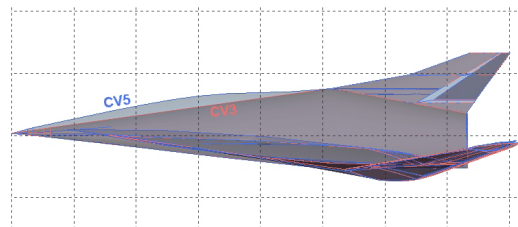


Figure 26. Fuselage changes to CV5 compared to CV3

The CV0 through CV5 Mach 0.3 AIRPLANE solutions were shown in Figure 4, and the Mach 6.0 AIRPLANE solutions were shown in Figure 5. Figure 27 shows a 3-view and an isometric view of the CV5 configuration.

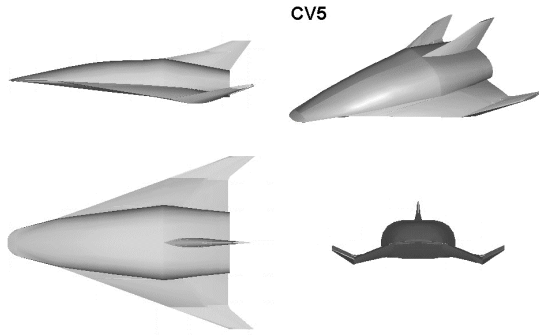


Figure 27. Rapid redesign configuration, CV5

From the results of the computational simulations, a new function table for CV5 was generated and implemented into the simulation. In addition, the control system was optimized using the same specifications as the previous 5 CTV configurations. The pilot evaluations yielded Level 1 handling qualities ratings for CV5 for all specified tasks during the approach and landing as shown in Figure 25.

In conclusion, the VMS simulation experiment was successful in obtaining Level 1 handling qualities ratings for 5 of the 6 CTV configurations (CV0 through CV5 except CV4). The experiment was also successful in obtaining handling qualities ratings for the Space Shuttle Orbiter and HL-20 simulations for comparison purposes. The experiment also provided enough pilot feedback to help establish good design specifications for the control system optimization tool. Finally, the re-design case was successful in demonstrating that the RITE tools and processes are capable of rapidly changing the vehicle design and obtaining handling qualities from a piloted simulation.

### Summary

The Virtual Flight Rapid Integration Test Environment project has demonstrated the capability of integrating CFD, flight and wind-tunnel data into a simulation rapidly and seamlessly. The goal of this project was to develop a design environment that merges these technologies and data to meet the challenges of

designing air and space vehicles. The objectives, to reduce the design cycle time, and to maximize the performance and utilization of these current resources, were met. A design of a Crew Transfer Vehicle concept was developed using this process. An information technology process and infrastructure was created to facilitate the integration and selection of the data. A simulation experiment, conducted in the NASA Ames VMS facility, evaluated the low-speed handling qualities of the various configurations in the approach and landing phase. Six astronaut pilots evaluated each of the configurations using Cooper-Harper ratings. The knowledge gained from the simulation data and pilot evaluations were quickly returned to the design team. From these findings, a new configuration was developed and cycled back through the simulation evaluation. The results and findings from this simulation experiment were presented. The details of this integrated design process along with the six resulting CTV configurations (CV0 through CV5) were also presented.

### Acknowledgements

The authors would like to thank the following NASA Johnson Space Center astronauts and Langley pilot for their support and participation in the VMS experiment. Special thanks to Kenneth Ham, Terrence Wilcutt, Steve Lindsey, Scott Horowitz, George Zamka, Chris Ferguson and Robert Rivers.

The authors would also like to thank the members of the Systems Analysis Branch and the Computational Sciences Division for their many contributions to the design and information technology process. Special thanks to Alex Te, Arsenio Dimanlig, Scott Thomas and Ray Hicks, all of the ELORET Corp., and Jorge Bardina of NASA Ames Research Center.

The authors would also like to thank Mark Tischler, Jack Franklin, Sean Swei and Kenny Cheung for their assistance with the CONDUIT optimization process.

Finally, special thanks to the members of the Simulation Division for their many contributions and operation of the VMS simulation experiment. Special thanks to Joseph Ogwell, John Bunnell, Dan Wilkins and Christopher Sweeney, all of the Logicon Corp.

## References

1. *Shuttle Performance: Lessons Learned*, NASA Langley Research Center, NASA Conference Publication 2283, March 1983.
2. Jackson, E. B., Ragsdale, W.A., Powell, R.W., *Utilization of Simulation Tools in the HL-20 Conceptual Design Process*, AIAA Paper 91-2955, August 1991.
3. Rivers, R. A., Jackson, E.B., Ragsdale, W.A., *Preliminary Piloted Simulation Studies of the HL-20 Lifting Body*, Journal of Aircraft Vol. 31, No. 3, pp. 556-563, May-June 1994.
4. Kinney, D. J., Bowles, J.V., Yang, L.H. and Roberts, C.D., *Conceptual Design of a 'SHARP'-CTV*, AIAA Paper 2001-2887, June 2001.
5. Kolodziej, P., Bull, J., Salute, J. and Keese, D.L., *First Flight Demonstration of a Sharp Ultra-High Temperature Ceramic Nosetip*, NASA TM 112215, December 1997.
6. Saltzman, E. J., Wang, K.C. and Iliff, K.W., *Flight-Determined Subsonic Lift and Drag Characteristics of Seven Lifting-Body and Wing-Body Reentry Vehicle Configurations with Truncated Bases*, AIAA Paper 99-0383, January 1999.
7. Stone, H. W. and Piland, W. M., *21<sup>st</sup> Century Space Transportation System Design Approach: HL-20 Personnel Launch System*, AIAA Journal of Spacecraft and Rockets, 30(5):521-528, September-October 1993.
8. Totah, J. J., Kinney, D.J., Kaneshige, J.T., and Agabon, S., *An Integrated Vehicle Modeling Environment*, AIAA Paper 99-4106, 1999.
9. Aftosmis, M. J., Berger, M. J., and Melton, J. E., *Robust and Efficient Cartesian Mesh Generation for Component-Based Geometry*, AIAA Paper 97-0196, January 1997.
10. Baker, T. J., and Vassberg, J. C., *Tetrahedral Mesh Generation and Optimization*, Proceedings of the 6<sup>th</sup> International Conference on Numerical Grid Generation, International Society of Grid Generation (ISGG), Mississippi State Univ., 1998, pp. 337-349.
11. Jameson, A., Baker, T. J., *Improvements to the Aircraft Euler Method*, AIAA Paper 87-0452, January 1987.
12. Jespersen, D.C., Pulliam, T.H., and Buning, P.G., *Recent Enhancements to OVERFLOW*, AIAA Paper 97-0644, January 1997.
13. Meakin, R. L. and Wissink, A.M., *Unsteady Aerodynamic Simulation of Static and Moving Bodies Using Scalable Computers*, AIAA Paper 99-3302.
14. Miranda, L.R., Elliot, R.D. and Baker, W.M., *A Generalized Vortex Lattice Method for Subsonic and Supersonic Flow Applications*, NASA Contractor Report 2865, Contract NAS1-12972, December 1977.
15. Tischler, M.B., Colbourne, J. D., Morel, M. R., Biezad, D. J., Levine, W. S., and Moldoveanu, V., *CONDUIT - A New Multidisciplinary Integration Environment for Flight Control Development*, AIAA Paper 97-3773, August 1997.
16. Gill, P.E. Murray, W., and Wright, M.H., *Practical Optimization*, 4<sup>th</sup> ed., Academic Press, San Diego, 1982.
17. Cooper, G.E., and Harper, R.P., Jr., *The Use of Pilot Rating in the Evaluation of Aircraft Handling Qualities*, NASA TN D-5153, April 1969.
18. Zilliac, G. G., and Clifton, E.W., *Wind Tunnel Study of an Observatory Dome with a Circular Aperture*, NASA TM 102888, November, 1990.
19. United States Department of Defense, *Flying Qualities of Piloted Vehicles*, MIL-STD-1797, 1987.